Available online at www.sciencedirect.com

ScienceDirect

journal homepage: www.elsevier.com/locate/issn/15375110

Research Paper

Quantifying the role of weather forecast error on the uncertainty of greenhouse energy prediction and power market trading

Henry J. Payne [a,*], *Silke Hemming* [b], *Bram A.P. van Rens* [c], *Eldert J. van Henten* [a], *Simon van Mourik* [a]

[a] *Farm Technology Group, Wageningen University, Wageningen, the Netherlands*
[b] *Greenhouse Horticulture, Wageningen University and Research Centre, Wageningen, the Netherlands*
[c] *Blue Radix B.V, P.O. Box 10075, 3004 AB Rotterdam, the Netherlands*

ARTICLE INFO

Article history:
Received 9 December 2021
Received in revised form
14 September 2022
Accepted 26 September 2022

Keywords:
Greenhouse horticulture
Statistical uncertainty
Weather forecasting
Energy efficiency
KASPRO

Currently the Dutch greenhouse horticultural sector has a high energy demand. The present use of weather forecasts can exacerbate this high energy consumption by contributing to suboptimal prediction and trading of the greenhouse's power demand. This study investigates the role of weather forecast errors on energy prediction power and trading uncertainty in greenhouse horticulture. This was done using an uncertainty analysis and computer model of a tomato producing Venlo style greenhouse in Bleiswijk, The Netherlands. This greenhouse model was used to predict the greenhouse's gas and electrical power demand. The study concluded that errors in the weather forecast of outdoor radiation, temperature and wind speed caused an overestimation of greenhouse energy demand. A sensitivity analysis showed that the radiation forecast error had the greatest impact on predicted greenhouse power demand errors with a mean relative error of 6.1%. Predicted gas demand errors were most dependent on the outside wind speed forecast mean relative error (18.0%) and temperature forecast error (17.2%). A power trading uncertainty analysis was done to investigate the impact of predicted energy demand errors on the cost of buying power on the Dutch imbalance and Amsterdam Power Exchange day-ahead market. This cost analysis found that the volume of initial power trading was greater than corrective trading. Additionally, the higher volatility in short term power prices resulted in higher corrective power costs per unit of power than if the power demand had been initially predicted with more accuracy.

* *Corresponding author.*
E-mail address: henry.payne@wur.nl (H.J. Payne).
https://doi.org/10.1016/j.biosystemseng.2022.09.009

Nomenclature

$c_{p,air}$	Specific heat capacity of air (J kg^{-1})
C_D	Cost of initial power demand prediction (€ h^{-1})
C_I	Cost of corrective power demand prediction (€ h^{-1})
d	Number of forecasts
h	Hourly time step (h)
H_{AirCov}	Heat flux between the main compartment air and cover (W m^{-2})
H_{AirFlr}	Heat flux between the main compartment air and floor (W m^{-2})
H_{AirOut}	Heat flux between the main compartment air and outside air (W m^{-2})
H_{AirScr}	Heat flux between the main compartment air and screen (W m^{-2})
H_{AirTop}	Heat flux between the main compartment air and the top compartment air (W m^{-2})
H_{CrpAir}	Heat flux between the main compartment air and the canopy level air (W m^{-2})
H_{LowAir}	Heat flux between the main compartment air and the lower heating pipe (W m^{-2})
H_{UppAir}	Heat flux between the main compartment air and the upper heating pipe (W m^{-2})
M_H	Molar mass of water (kg mol^{-1})
P_{AluAir}	Heat flux with the lamps (W m^{-2})
P_D	APX day-ahead price (€ W h^{-1})
P_I	Imbalance price (€ W h^{-1})
P_{SunAir}	Heat flux incoming from the sun (W m^{-2})
Q	Forecast prediction horizon length (h)
R	Universal gas constant (J K^{-1} mol^{-1})
SI	Sensitivity indices
T_{air}	Indoor air temperature (°C h^{-1})
v_{air}	Greenhouse air volume (m^3)
V_{AirCov}	Water vapour flux between the main compartment air and the cover (kg h^{-1} m^{-2})
V_{AirOut}	Water vapour flux between the main compartment air and the outside air (kg h^{-1} m^{-2})
V_{AirScr}	Water vapour flux between the main compartment air and the screen (kg h^{-1} m^{-2})
V_{AirTop}	Water vapour flux between the main compartment air and the top compartment air (kg h^{-1} m^{-2})
V_{CanAir}	Water vapour flux between the main compartment air and the canopy level air (kg h^{-1} m^{-2})
VP_{air}	Main compartment water vapour pressure (Pa h^{-1})
Y^F	Energy prediction made with weather forecasts
Y^R	Energy prediction made with weather recordings
X^F	Forecast weather data
X^R	Recorded weather data
ΔY^1	The first order forecast error
ΔY^2	The second order forecast error
ε^F	Weather forecast error
ε^F_T	Total forecast error in a forecast period
$\varepsilon_{\%}$	Percentage prediction error (%)
ε^P	Energy prediction error
ε^P_{PT}	Accumulated energy demand over-prediction
ε^P_{NT}	Accumulated energy demand under-prediction
ρ_{air}	Air density (kg m^{-3})

1. Introduction

The Netherlands has a large greenhouse sector of approximately 10,554 ha (Statistics Netherlands [Internet], 2021), with a power demand of 110 PJ in 2020. This power annually costs the grower 6.5 € m^{-2} (van der Velden & Smit, 2021) on average making cost effective energy buying a priority. An industrial greenhouse is a highly complex system, and the grower may require frequent advice to achieve efficient management. This advice is used to supplement and computerise human expertise by predicting the greenhouse's future behaviour and offering appropriate climate management advice as shown in Fig. 1. Computer models and data streams are used to generate the advice and form part of a decision support system (DSS). The advice that this study focusses on is how much energy should be bought to operate the greenhouse. The external sources of energy being considered in this study are the gas and electrical power required by the greenhouse.

The predictive accuracy of a DSS is important as it allows the accurate planning and trading of power on the power markets (Wang, Mao, & Nelms, 2015). This greenhouse's future energy demand is predicted using the weather forecast and predicted energy prices (van Beveren, Bontsema, van't Ooster, van Straten, & van Henten, 2020). However, errors within the weather forecasts may affect the accuracy of predictions and the efficiency of subsequent energy trading.

In the Netherlands the greenhouse's predicted power demand is initially bought using the APX (Amsterdam Power Exchange) day-ahead power market. The day-ahead market allows bidders to submit an order for power at an hourly rate, which will be delivered the next day. Any errors in this initial purchase are resolved by using corrective power trading on the APX intra-day market or imbalance market. The intra-day market allows the continuous trading of power on an hourly rate, and the imbalance price is used to reflect the immediate value of power given the current ratio of supply and demand on the grid.

In previous greenhouse studies weather forecasts have been included in various forms. Some studies have used actual forecast data (Sigrimis, Ferentinos, Arvanitis, & Anastasiou, 2001; Su, Xu, & Goodman, 2021), and others include simplified forms of forecasts such as a lazy-man forecast (Tap, van Willigenburg, & van Straten, 1996; van Ooteghem, 2010). Some studies create synthetic forecasts using models (Seginer, van Beveren, & van Straten, 2018; Su, Xu, & Goodman, 2017a).

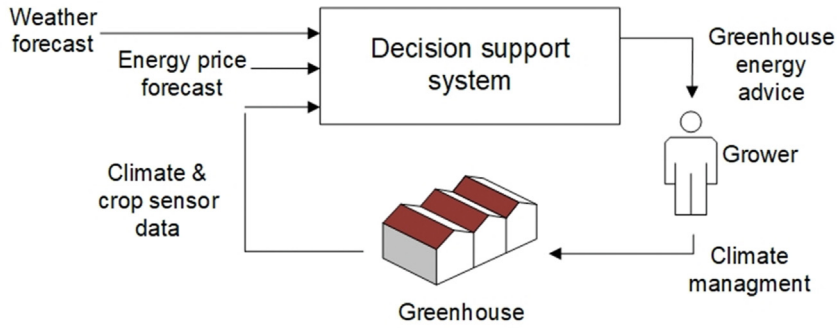

Fig. 1 – A flow diagram of how a greenhouse decision support system connects sensor data, forecast data and the grower, and how advice on greenhouse energy consumption may be applied in the greenhouse.

Several studies that have focused on greenhouse energy management have included weather forecasts. Among these some address reducing the greenhouse's heating demand (Chalabi, Bailey, & Wilkinson, 1996; Su et al., 2021) or heating costs (Gutman, Lindberg, Ioslovich, & Seginer, 1993). Keesman, Peters, and Lukasse (2003) investigates the reduction of ventilation costs in a potato storage facility using a receding horizon optimal controller and weather forecasts. However in these studies and several other studies it is assumed that the errors in weather forecasts have a negligible effect on the prediction accuracy of greenhouse models (Seginer, Ioslovich, & Albright, 2006; Seginer & McClendon, 1992).

The potential impact of weather forecast errors on greenhouse prediction uncertainty has been partially addressed. Vogler-Finck, Bacher, and Madsen (2017) use a simple linear model and a recursive least squares approach to predict the heat demand of a Danish greenhouses using short term weather forecasts. Vogler-Finck concluded that the inclusion of real weather forecasts significantly improved the online prediction of heat load over using simplified weather forecasts. Tap et al. (1996), studied the greenhouse's CO_2 and heating demand and simulated the financial performances of a greenhouse model being controlled with a receding horizon optimal controller. Tap et al. (1996) found a drop in the performance of a greenhouse when forecast errors were introduced, and that the performance worsened for longer forecasts. Doeswijk, Keesman, and Van Straten (2006) also found that weather forecast errors increase the heating costs of operating a climate controlled storehouse. Sigrimis et al. (2001) offer a nuanced perspective by concluding that while the inclusion of weather forecasts can improve performance, the presence of weather forecast errors increased the costs of heating and that this cost only worsened with longer forecasts.

As shown above the error within weather forecasts previous research has analysed in the context of greenhouse heating control and economic optimisation. However, there is a knowledge gap as there are limited studies about the effects of weather forecast error on power demand prediction and the subsequent consequences for power trading.

Several studies optimised the cost of the of the greenhouse's energy usage (Golzar, Heeren, Hellweg, & Roshandel, 2021; Seginer, van Straten, & van Beveren, 2017; Vadiee & Martin, 2012; van Beveren, Bontsema, van Straten, & van Henten, 2019; van Henten & Bontsema, 2009; Vanthoor et al., 2012) and several studies have included weather forecasts (Doeswijk et al., 2006; Gutman et al., 1993; Keesman et al., 2003; Sigrimis et al., 2001; Tap et al., 1996). However, many studies are limited in how realistic they are when compared to what is done in practice as the economics of the greenhouse were often significantly simplified. For example a fixed power price is often used (Golzar et al., 2021; Kuijpers et al., 2021; Vadiee & Martin, 2012; Vanthoor et al., 2012). van Beveren et al. (2019) did include a fluctuating price by optimising the use of the greenhouse's energy equipment using the imbalance price. However as discussed above, this is not what is done in practice.

Many studies have optimised the economics of a greenhouse by using simplified market prices to assess the greenhouse's economic performance. As a result, there is an additional knowledge gap as little information is available on the potential costs of power trading using fluctuating prices and multiple markets as is done in the greenhouse horticulture sector.

The objective of this paper is to determine the impact of weather forecast error on greenhouse energy demand prediction and power trading. In addition, this study investigated which forecast variables have the greatest impact on power prediction error and how this impact changes depending on the weather forecast prediction horizon length.

By identifying the roles of the error in weather forecast variables, improvements can be made to the most error prone variables through the targeted application of improved sensors or by using combinations of multiple forecasts. This in turn can improve the accuracy of energy demand prediction and the economic efficiency of power trading.

In the subsequent sections the greenhouse model is briefly described. This is followed by an uncertainty analysis that describes the error in the weather forecast and how that propagates into uncertainty in the energy demand prediction. Next the uncertainty in the energy demand prediction was used to calculate the costs of power trading when trading on the APX day-ahead and imbalance markets. A local sensitivity analysis was then done to assess which weather forecast variable's errors are having the greatest impact on prediction uncertainty. The results are then interpreted to focus on the impact weather forecast errors have on energy prediction and trading. Moreover, this study aims to assess how this impact

changes when using weather forecasts of differing prediction horizon lengths.

This paper makes a novel contribution to the field of greenhouse horticultural modelling by investigating the propagation of weather forecast error into predicted greenhouse energy demand and power trading. The novelty of this work consists of the following features:

- This study takes a detailed approach to assessing the costs of buying the greenhouse's power demand. This demand is calculated initially using the APX day-ahead power market price, which is a realistic representation of the initial and largest round of trading done by growers in practice in the Netherlands. Then the cost of the mispredicted power is calculated using the imbalance market price to represent the costs of short-term corrective trading.
- The application of this input data-based uncertainty analysis in the greenhouse horticulture domain is novel and in particular the application of a weather forecast based uncertainty analysis within the greenhouse domain.
- Unlike previous sensitivity analysis methods in the greenhouse modelling domain which focused on the sensitivity of parameters, this study uses an input data discrete sensitivity analysis which is applied on the weather variables to determine the largest contributors to the energy prediction uncertainty.

2. Materials and methods

2.1. Model definition

The greenhouse model used in this study is composed of modules (Fig. 2) which are described in the following subsections. This study uses the greenhouse model KASPRO (de Zwart, 1996; Dieleman, Meinen, Marcelis, de Zwart, & van Henten, 2005; Elings, de Zwart, Janse, Marcelis, & Buwalda, 2006; Luo, de Zwart et al., 2005; Luo, Stanghellini, et al., 2005) which is extensively calibrated to represent a commercial Venlo type Dutch greenhouse. For clarity of explanation the KASPRO model is described as being divided into modules which simulate the operation of the indoor greenhouse climate, energy system and rule-based controller. The energy asset control action is the response of the controller to activate the greenhouse energy assets (CHP, Boiler, lamps, screens, and ventilation). The climate control action defines the heating, lighting and CO_2 input to the greenhouse climate from the energy assets.

2.2. Greenhouse climate module

The climate module models the indoor climate of the top and main compartments of the greenhouse and includes 16 state variables, including the indoor air temperature, carbon dioxide concentration, and vapour pressure. The greenhouse

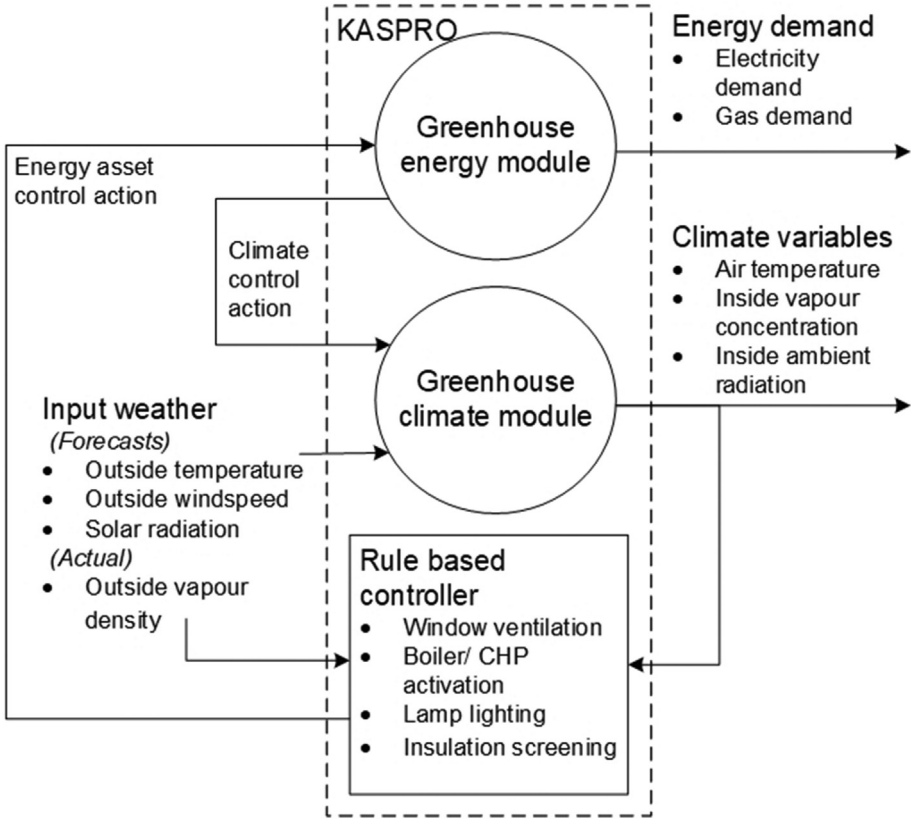

Fig. 2 – This figure shows the relations of the modules within the KASPRO greenhouse model and the role of weather data.

climate module (Fig. 2) receives input data from the outside weather and the energy input to the climate from the energy module. Figure 3 shows the relative position of the elements in the greenhouse and their relation to the top and main compartments. This includes the air above and below the thermal screen, at the greenhouse cover and crop canopy level, as well as in six layers of soil. The elements displayed in this figure are not to scale. The transfer of water vapour, CO_2 and energy between elements of the greenhouse are governed by the processes of radiative and latent heat exchange, conduction, convection, ventilation, and condensation.

This study focusses on the states in the model describing the indoor air temperature and water vapor pressure in the main compartment in the form of differential equations (Eqs. (1) and (2)). The insight gained from the model's indoor air CO_2 state (de Zwart, 1996) was not used in this paper as the relevant outdoor CO_2 data was unavailable. The implications of this limitation are examined using a sensitivity analysis described in Appendix A.

The main compartment temperature (Eq. (1)) (de Zwart, 1996) is scaled by a fraction of air density (ρ_{air}), specific heat capacity of air ($c_{p,air}$) and the volume of air (v_{air}). This is then multiplied by the net energy being transferred between the regions of the greenhouse, composed of the heat gained from the artificial lights (P_{AluAir}) and solar radiation (P_{SunAir}), upper and lower heating pipes (H_{UppAir}, H_{LowAir}) and the canopy air(H_{CrpAir}). Also included are the heat lost to the floor (H_{AirFlr}), top compartment (H_{AirTop}), shade screen (H_{AirScr}), thermal cover (H_{AirCov})and the outside (H_{AirOut}).

$$\frac{dT_{air}}{dt} = \frac{1}{\rho_{air} \bullet c_{p,air} \bullet v_{air}} * \left(P_{AluAir} + P_{SunAir} + H_{UppAir} + H_{LowAir} + H_{CrpAir} - H_{AirFlr} - H_{AirTop} - H_{AirScr} - H_{AirOut} - H_{AirCov}\right) \left[\circ Ch^{-1}\right] \quad (1)$$

Within the model the main compartment vapour pressure state (Eq. (2)) (de Zwart, 1996) is defined as a fraction of the water molar mass (M_H), the gas constant (R), the volume of air (v_{air}) and the main compartment air temperature (T_{air}). This was then multiplied by the sum of the vapour released from the canopy (V_{CanAir}) and lost to the top compartment, screen, cover and outside ($V_{AirTop}, V_{AirScr}, V_{AirCov}, V_{AirOut}$).

$$\frac{dVP_{air}}{dt} = \frac{1}{M_H \bullet \frac{v_{air}}{R \bullet T_{air}}} \bullet \left(V_{CanAir} - V_{AirTop} - V_{AirScr} - V_{AirCov} - V_{AirOut}\right) \times \left[Pah^{-1}\right] \quad (2)$$

For the purposes of this study a representative greenhouse design was specified. This greenhouse is a Venlo type greenhouse producing tomato in Bleiswijk, Netherlands. The physical parameters of the greenhouse are shown in Table 1.

2.3. Greenhouse energy module

The greenhouse energy module receives the data describing the use of energy system components from the rule-based controller. The energy module describes the amount of pipe heating, lamp lighting and injected CO_2 input into the

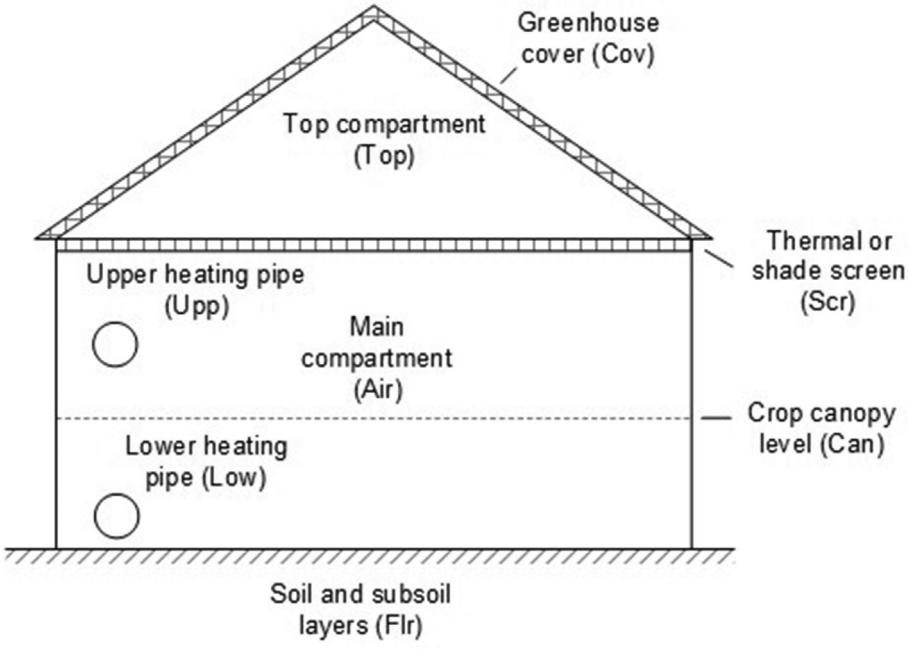

Fig. 3 – This figure shows a cross section of the modelled Venlo type greenhouse. The figure describes the location of the greenhouse elements (screens, covers and pipes) within the greenhouse compartments as described in the KASPRO greenhouse model. The elements in this figure are not to scale but shows their relative positions in the greenhouse and abbreviations.

Table 1 – Parameters of the simulated greenhouse structure.

Property	Value	Units
Footing area	2.4	ha
Total height	6.5	m
Number of windows	1200	~
Number of chambers	1	~
Gutter height	6	m
Cladding area	27,000	m^2
Window size	2.5 × 1.2	m
Upper heating pipe diameter	0.027	m
Lower heating pipe diameter	0.051	m
Number of lower heating pipe per floor area	1.25	Pipes m^{-2}
Number of upper heating pipe per floor area	0.625	Pipes m^{-2}

greenhouse climate as well as the required gas and power to operate the components of the energy system. These components include a shading and energy screens. Heating was supplied via a lower and upper heating rail pipe system from a boiler, combined heat and power generator (CHP) and heat storage tank. Lighting was supplied from two arrays of SON-T 1000 W HPS (High Pressure Sodium) lamps. The greenhouse energy system components properties are listed in Table 2.

2.4. Rule-based controller

The rule-based controller module receives data from the outside weather and the indoor greenhouse climate and outputs the usage of greenhouse energy assets to meet predefined indoor climate conditions (Luo, de Zwart et al., 2005). The use of energy assets was defined as the immediate fraction of window aperture, fraction of lamp lighting levels and fraction of insulation screen coverage. The controller also dictates the temperature of the greenhouse heating system via the control of the CHP and boiler.

The controller resembles an industrial grade controller which operates from a considerable library of threshold-based rules. The threshold values were defined by climate profiles which detail desired climate conditions as a series of set points over time, as well as the time, outside weather and the actual indoor climate.

Table 2 – Properties of the greenhouse energy system components relating to the capacity of the components, and efficiency of energy assets.

Property	Value	Units
Lower heating pipe diameter	51	mm
CHP power rating	43	Wm^{-2}
CHP thermal capacity	60	Wm^{-2}
Artificial light intensity	0.648	mol $m^{-2}h^{-1}$
Upper heating pipe diameter	27	mm
CHP heating efficiency	47	%
Boiler thermal capacity	170	Wm^{-2}
Heat tank volume	1000	m^3
Boiler heating efficiency	94	%
CHP electrical efficiency	37	%

The climate profile used in this study has a relative humidity set point of 85% and a requirement to light the greenhouse for 18 h a day ending at 20:00. The temperature climate profile has set points of 18°C between sunset and sunrise, 20°C 1 h after sunrise, 19°C 1 h before sunset. For consistency over the simulations the climate set point scheme was kept the same for all weather forecast prediction horizon lengths.

2.5. Model assumptions

The greenhouse climate and energy system model were implemented with some simplifications and assumptions. Key simplifications and assumptions are listed below:

- The greenhouse compartments are homogeneous spaces, with no spatial microclimate variation within them.
- The effects of shadow screens, covers, ventilation windows and artificial lighting on state variables are uniform within their related regions of the greenhouse.
- The flow of water through the heating system was assumed to be constant over time.
- KASPRO (de Zwart, 1996; Dieleman et al., 2005; Elings et al., 2006; Luo, de Zwart et al., 2005; Luo, Stanghellini, et al., 2005) is an extensively calibrated model and it is assumed that this calibration makes it a sufficiently representative predictor.
- It is assumed that the predictions made using the weather recordings represent a ground truth to be compared with the weather forecasts. This is necessary as it is not possible to record the performance of a real greenhouse that operates using forecasts with no error as no such forecasts exist.

2.6. Power market data

The cost of power trading in this study was calculated using the Netherlands APX day-ahead and the imbalance market price for power over the same period as the forecast data. The APX day-ahead market was chosen as it represents the prices upon which the majority of initial energy trading is done for growers. The APX price data is applied in an uncertainty analysis along with weather forecast data. This is done to represent a medium-term energy planning scenario over multiple days. To calculate the costs of corrective power trading that is done based on the mispredicted power demand the imbalance market price is used. The imbalance price was chosen over the intra-day market due to the lack of availability of intra-day market data. In this study it is assumed that the volumes of power traded by the grower do not affect the market price.

2.7. Recorded and forecasted weather data

A dataset of hourly weather forecasts and weather recordings is used in this study. The dataset includes hourly forecast and recording variables of the outside temperature (°C), wind speed (ms^{-1}) and global solar radiation (Wm^{-2}). The forecasts

have a five-day length and were generated at: 06:00, 09:00, 12:00, 15:00 and 17:00 over a two-month period (13 Oct 2019–16 Dec 2019), resulting in 292 five-day forecasts in total. The forecasts were generated by the weather forecast company Meteoconsult and was sourced from an operational greenhouse and is comparative to what information is available to growers.

The forecasts of outside vapour concentration (gm^{-3}) were not included in the original data set. In place of these forecasts, recordings were retrieved from a nearby KNMI (Koninklijk Nederlands Meteorologisch Instituut) meteorological station for the same period of time were used in place of a forecast. The outdoor $C0_2$ concentration for both the weather forecast and recordings was assumed to be constant at 410 ppm, the impact of this assumption is examined in appendix A.

In addition, the cloudiness index (CI) was fixed to the average of the period (CI = 0.7). A sensitivity analysis found that this assumption has little impact on the study's result, the results of which can be seen in Appendix A. The sky temperature (Luo, de Zwart et al., 2005) and levels of diffused radiation (Orgill & Hollands, 1977) were computed using the available climate variables. Any missing entries in the datasets were filled with the value at the previous time instance, this was done for simplicity.

2.8. Uncertainty analysis method

This study uses a method that is described in four sections. These sections describe the method used to compose the weather forecasts, and to explain the uncertainty in the weather forecast, energy prediction and power trading respectively. The steps of the method, their relations, key variables, and sections are shown in Fig. 4. This study analyses the effect of using weather forecasts of increasing length (Q), from 1 to 5 days long at daily intervals. This study defines uncertainty analysis as the analysis of a distribution of errors.

2.8.1. Compose weather forecast series

This study uses series of weather forecasts with a horizon length in hours (Q), where $Q = [24, 48, 72, 96, 120]$. These horizon lengths are indexed through using $i = 1..i_{max}$, where $i_{max} = 5$. For each weather forecast horizon length and forecast starting time, a series of consecutive forecasts (X^F) was used. This series of forecasts spanned the time period of the entire data set. Due to 5-day forecasts being recalculated daily, it is possible to concatenate forecasts with periods shorter than 5 days. This was done by truncating the weather forecasts from their starting sample to the given horizon length.

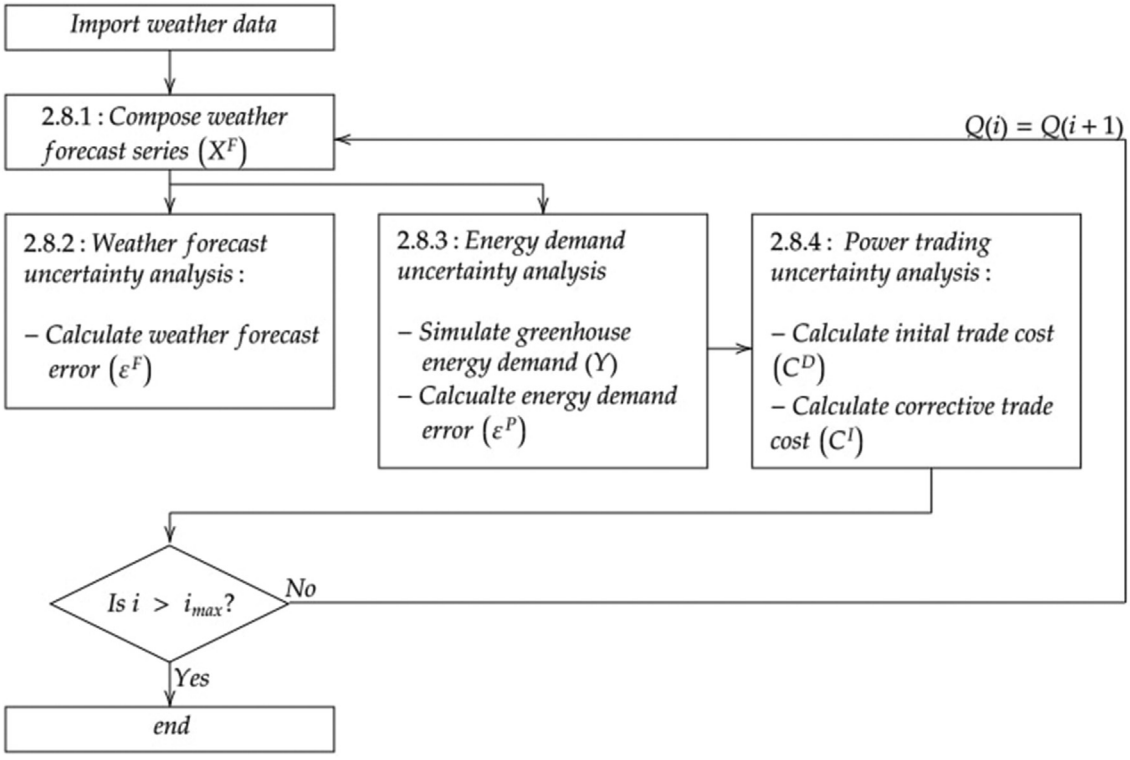

Fig. 4 – The steps for the analysis method used in this study and the corresponding sections of the manuscript. Each step in the figure includes title of the step, the corresponding section of the manuscript and the key variable from that step. This method is iterated through each forecast prediction horizon length (Q) using the index i.

2.8.2. Weather forecast uncertainty analysis

To investigate the role of weather forecast uncertainty on greenhouse energy prediction uncertainty, a sample based uncertainty propagation method is adapted and applied (van der Meer, Widén, & Munkhammar, 2018). In this study time in is discretised using hourly time steps and each time interval is defined by its length in hours, $Q(i)$, and starting point (d,h), where d is the day of the year, and h is the hour in the day. The hourly forecast error $(\varepsilon^{F}_{Q(i)}(d,h))$ at each time instance is defined as the difference between the weather recording $(X^{R}_{Q(i)}(d,h))$ and forecasts $(X^{F}_{Q(i)}(d,h))$:

$$\varepsilon^{F}_{Q(i)}(d,h) = X^{F}_{Q(i)}(d,h) - X^{R}_{Q(i)}(d,h) \tag{3}$$

These errors were then summed (ε^{F}_{T}) as this represented the quantity of error made over a forecast period, such that,

$$\varepsilon^{F}_{T}(d) = \sum_{h=1}^{Q(i)} \varepsilon^{F}_{Q(i)}(d,h) \tag{4}$$

2.8.3. Energy demand uncertainty analysis

The energy prediction error is calculated as the difference between predictions calculated using weather forecasts and predictions made with weather recordings for the same period. The energy demand predictions Y from the model includes the gas demand Y_G $(m^3m^{-2}h^{-1})$ and power demand Y_P $(Wm^{-2}h^{-1})$ where $Y = [Y_P\ Y_G]^T$. The greenhouse energy demand $(Y^{F}_{Q(i)})$ is calculated using the KASPRO model over a period $Q(i)$, with inputs equal to the forecasted weather data (X^{F}). This results in predicted energy demand as a function of forecasted data,

$$Y^{F}_{Q(i)}(d,h) = Y\left(X^{F}_{Q(i)}(d,h)\right) \tag{5}$$

Then the energy demand $(Y^{R}_{Q(i)})$ is calculated using the recorded weather data (X^{R}) as input,

$$Y^{R}_{Q(i)}(d,h) = Y\left(X^{R}_{Q(i)}(d,h)\right) \tag{6}$$

The hourly prediction error $(\varepsilon^{P}_{Q(i)})$ is calculated by comparing the weather forecast and weather recording based energy predictions. Where

$$\varepsilon^{P}_{Q(i)}(d,h) = Y^{F}_{Q(i)}(d,h) - Y^{R}_{Q(i)}(d,h) \tag{7}$$

To avoid having the prediction errors cancel each other out the positive and negative error are summed for each forecast period $(Q(i))$ to represent the accumulated over-prediction (ε^{P}_{PT}) and accumulated under-prediction (ε^{P}_{NT}) respectively. Such that,

$$\varepsilon^{P}_{PT}(d) = \sum_{h=1,\varepsilon^{P}(d,h)>0}^{Q(i)} \varepsilon^{P}_{Q(i)}(d,h), \text{and} \tag{8}$$

$$\varepsilon^{P}_{NT}(d) = \sum_{h=1,\varepsilon^{P}(d,h)<0}^{Q(i)} \varepsilon^{P}_{Q(i)}(d,h) \tag{9}$$

The initially predicted energy demand $(Y^{F}_{Q(i)})$ and mispredicted energy demand $(\varepsilon^{P}_{Q(i)})$ are summed to allow a direct comparison of the quantity of error made over a forecast period, where,

$$Y^{F}_{T}(d) = \sum_{h=1}^{Q(i)} Y^{F}_{Q(i)}(d,h) \tag{10}$$

$$\varepsilon^{P}_{T}(d) = \sum_{h=1}^{Q(i)} \varepsilon^{P}_{Q(i)}(d,h), \text{and} \tag{11}$$

2.8.4. Power trading uncertainty analysis

This study investigates the financial consequences of power demand misprediction. These consequences are dependent on the volume of misprediction and the price of power on the markets it is being traded on. The hourly APX day-ahead market price (P^{D}) was used to calculate the power cost $(C^{D}_{Q(i)})$ of the initially predicted energy demand $(Y^{F}_{Q(i)})$, where,

$$C^{D}_{Q(i)}(d,h) = P^{D}(d,h) * Y^{F}_{Q(i)}(d,h) \tag{12}$$

The cost of the corrective bidding $(C^{I}_{Q(i)})$ of the mispredicted energy $(\varepsilon^{P}_{Q(i)})$ is calculated using the imbalance market price (P^{I}) and

$$C^{I}_{Q(i)}(d,h) = P^{I}(d,h) * \varepsilon^{P}_{Q(i)}(d,h) \tag{13}$$

To analyse and display the distribution of costs the matrices are concatenated into a vector. It should be noted that the power that can be generated and sold from the combined heat and power generator (CHP) is not considered in this study. This analysis does not consider the cost of gas demand as it is often fixed by contract unless a maximum supply rate is exceeded, which is assumed to be the case.

2.9. Sensitivity analysis of energy demand predictions

To understand which weather variable's forecast has the greatest effect on the predicted power and gas demand (Y) a local discrete sensitivity analysis was performed. This sensitivity analysis was done on the forecast and recorded weather variables which include, outdoor temperature, global radiation and wind speed. The first order error (ΔY^{1}) of each weather forecast variables are calculated (X^{F}_{k}). Each weather forecast variable is in turn used to replace the corresponding recorded weather variable and applied to calculate the energy demand predictions with the remaining recorded weather variables (X^{F}_{j}). The index k is the index of each weather forecast variable and j is the index of the remaining weather variables. Such that

$$\Delta Y^{1}_{k}(d,h) = Y\left(X^{R}(d,h)\right) - Y\left(X^{F}_{j}(d,h), X^{F}_{k}(d,h)\right) \tag{14}$$

where all the weather forecast variables were made equal to the recorded variables, except index k:

$$X^{F}_{j} = X^{R}_{j}, j \neq k \tag{15}$$

The second order error interactions (ΔY^{2}) is calculated by replacing pairs of weather forecast variables $(X^{F}_{m,n})$ to assess their combined influence. Where,

$$\Delta Y^{2}_{m,n}(d,h) = Y\left(X^{R}(d,h)\right) - Y\left(X^{F}_{j}(d,h), X^{F}_{m,n}(d,h)\right) \tag{16}$$

where

$$X^{F}_{j} = X^{R}_{j}, j \neq n, j \neq m \tag{17}$$

where m and n are the indexes of all pairs of weather

forecast variables. To allow comparison between predicted gas and power demand the percentile prediction error ($\varepsilon_{\%}$) was then calculated for the first and second order errors, accordingly

$$\varepsilon_{\%}^{\{1,2\}}(d) = \frac{\sum_{h=1}^{Q}\left(\Delta Y^{\{1,2\}}(d,h)\right)}{\sum_{h=1}^{Q}\left(Y\left(X^{R}(d,h)\right)\right)} * 100 \quad (18)$$

This percentile prediction error was then used to calculate the first and second sensitivity indices (SI) which is defined as the average absolute percentage error,

$$SI = \overline{|\varepsilon_{\%}(d)|} \quad (19)$$

3. Results

The results describe the effect of weather forecast uncertainty on energy use predictions and are split into four sections. The first section assesses the uncertainty in weather forecast variables. The second section shows the effect of the weather forecast error on greenhouse model prediction uncertainty and how it changes with the length of the weather forecast prediction horizon. The third section includes a power trading uncertainty analysis using multiple markets and weather forecast prediction horizon lengths. The last section investigates the interrelations between the input weather data and energy predictions using a discrete sensitivity analysis.

3.1. Weather forecast uncertainty

Figure 5 presents the total weather forecast errors (Eq. (4)) within each forecast variable for an increasing forecast horizon length. For all the forecast variables the mean error becomes more negative, and the variance increases as the horizon increases. This means that on average the forecast consistently underestimates the available outside temperature, global radiation and wind speed.

3.2. Greenhouse gas and power demand uncertainty

The greenhouse gas and power demand were simulated using different weather forecast prediction horizon lengths. Figure 6 shows that as the forecast horizon increases the variance and mean of the over and under-predicted power and gas increases. In addition, the amount of over-predicted power and gas is greater than the under-predicted amount in both mean and variation. Subsequently in this case the greenhouse model tends to overestimate the power and gas demand. This originates from the bias present in the weather forecasts, namely, in the case of power demand, a negative bias in the global radiation forecast error (Fig. 5), meaning too little natural light is being forecast. This result is also reflected in the sensitivity results shown in Section 3.4.

3.3. Greenhouse power trading uncertainty analysis

A comparison between the prices of the APX day-ahead and imbalance market is shown in Fig. 7. The comparison shows that the day-ahead price has a higher mean price than the imbalance price. However, the imbalance price has a far longer tail than the day-ahead price where extreme prices can occur. In addition, the day-ahead price is strictly positive during this period, and the imbalance price ranges over both positive and negative values.

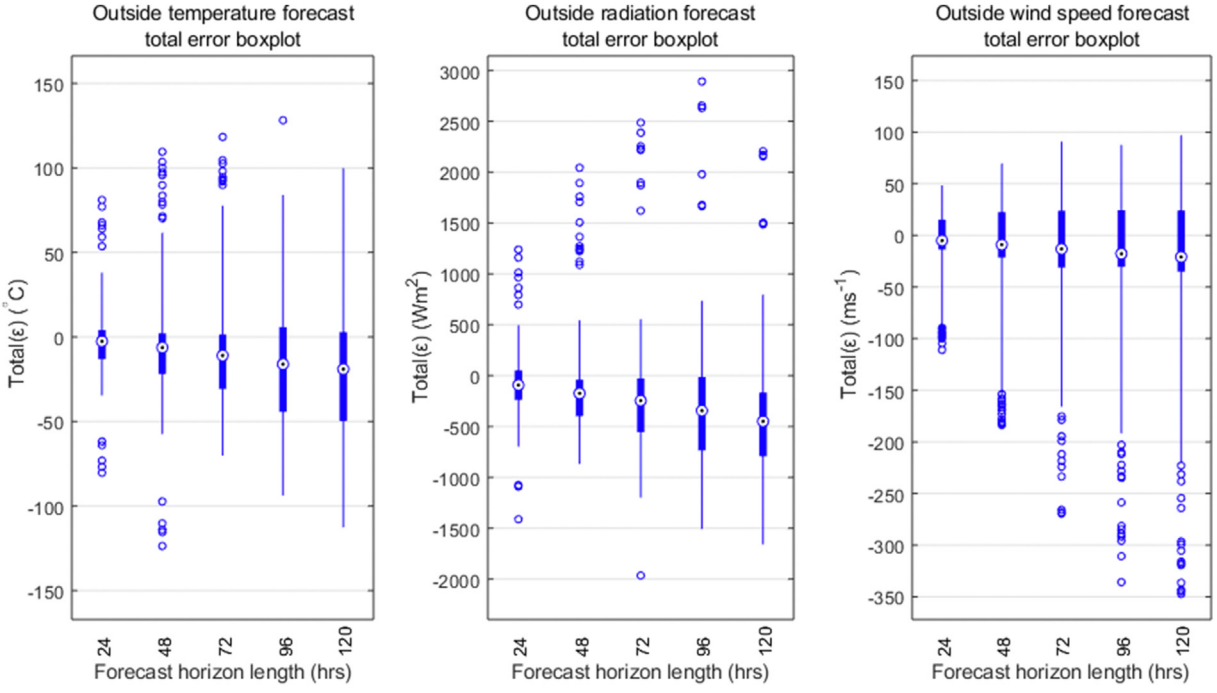

Fig. 5 – Boxplots of the total weather forecast errors (Eq. (4)) made over the forecast prediction horizon forecast length (Q). Where the encircled point is the mean, the box is the 1st, the whiskers are the 2nd standard deviations, and the open circles are the outliers.

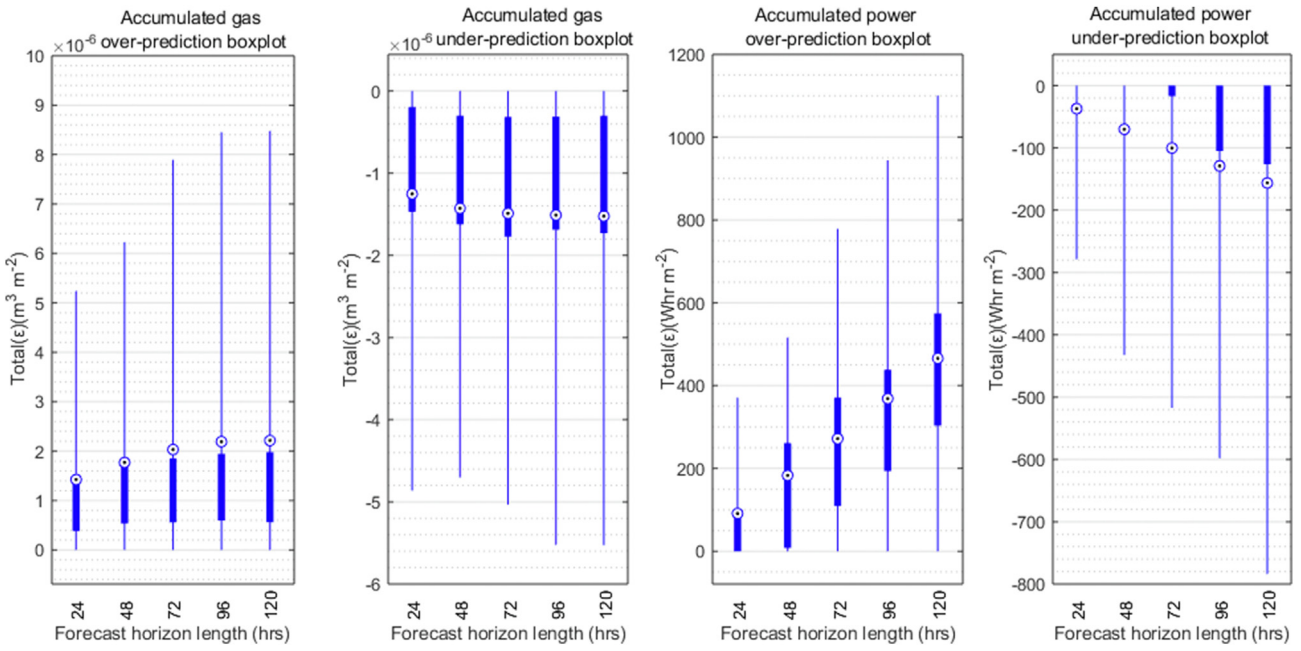

Fig. 6 – Boxplot distributions of the accumulated over and under prediction (Eqs. (8) and (9)) of gas and power demand when using forecasts of different forecast prediction horizon lengths. Where the encircled point is the mean, the box is the 1st and the whiskers are the 2nd standard deviations (outliers omitted for clarity).

Figure 8 shows the total volume of the initial and corrective power demand prediction of a forecast period (Eqs. 10 and 11). The total volume of the initially predicted demand is much greater than the corrective demand for all weather forecast prediction horizon lengths. For both the initial and corrective demand the mean increases, and the standard deviation decreases with the weather forecast prediction horizon length. In addition, the initial and corrective demand has a positive bias for all the forecast prediction horizon lengths. To better look at the impact of misprediction on incurred costs only nonzero results are shown for the power demand and costs (Eqs. 12 and 13) displayed in Fig. 9.

The comparative costs of the initial and corrective trading are shown in Fig. 9 and are derived from Eqs. (12) and (13). The initial bid is the larger in mean cost than the corrective costs and increases in mean and standard deviations as the forecast prediction lengths increase. The corrective costs have a greater variation and increase in mean cost with the forecast prediction horizon lengths. The standard deviation of the corrective costs does rise to a peak at a 72 h forecast horizon before declining. The negative value of the corrective bid cost represents the grower being paid as an incentive to purchase power on the imbalance market. This can occur when there is a surplus of power on the grid.

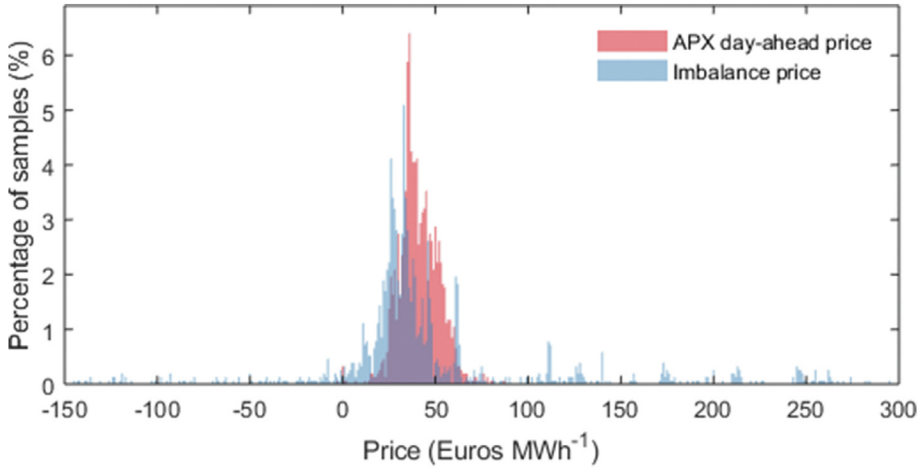

Fig. 7 – A histogram of the market prices on the APX day-ahead and imbalance power markets.

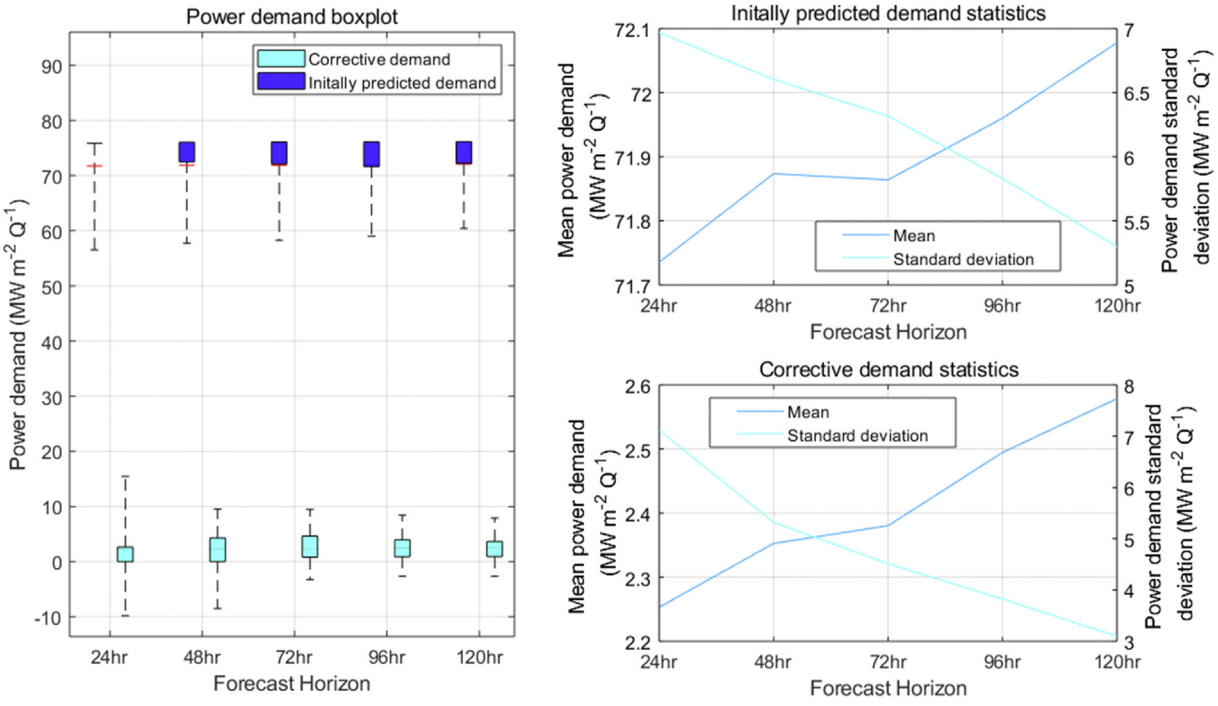

Fig. 8 – A boxplot (left) of the initially predicted power demand (Eq. (10)) and the subsequently calculated corrective power demand (Eq. (11)). These power demands are described as the total per forecast period Q. The mean and standard deviation for the initial and corrective demands (right) are displayed for each forecast prediction horizon length. Where the box is the 1st, and the whiskers are the 2nd standard deviations.

3.4. *Sensitivity analysis of greenhouse gas and power demand*

The sensitivity analysis shown in Fig. 10 is done using a 48-h weather forecast. This analysis revealed that the power demand prediction error is most related to the global radiation forecast error. The gas use prediction error is most related to the temperature forecast error, then the wind forecast error and marginally to the global radiation forecast error. Moreover, the error in gas prediction is highly sensitive

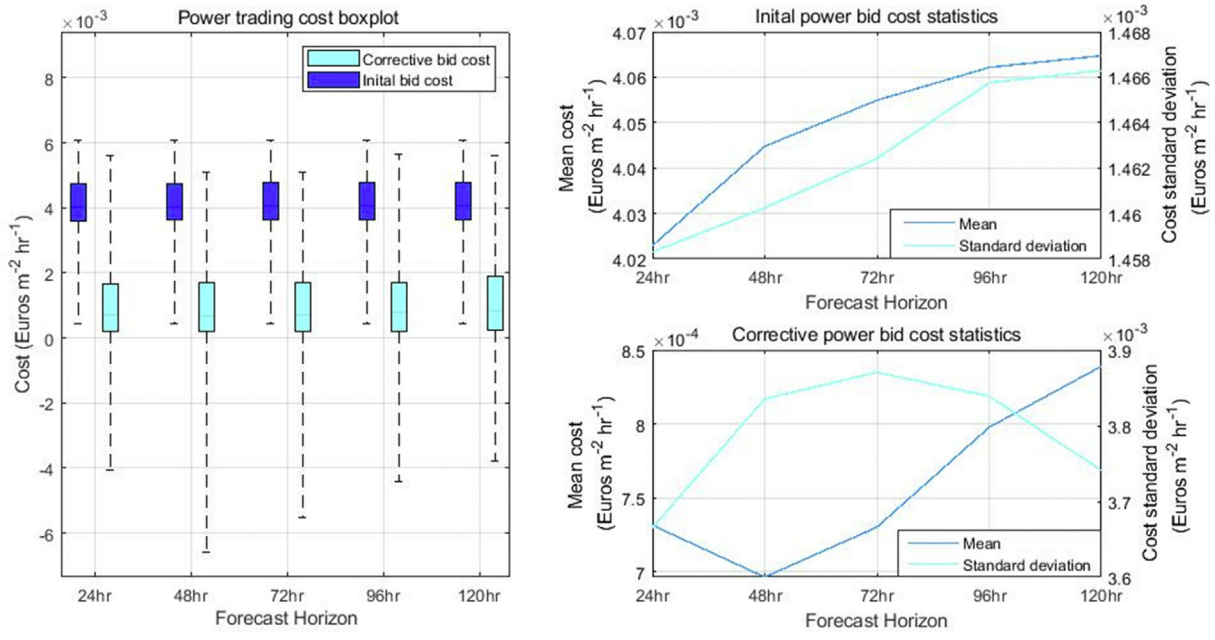

Fig. 9 – A boxplot (left) of the initial power costs (Eq. (12)) and the subsequently calculated corrective power costs (Eq. (13)). The mean and standard deviation for the initial and corrective demands (right) are displayed for each forecast prediction horizon length. Where the box is the 1st, and the whiskers are the 2nd standard deviations.

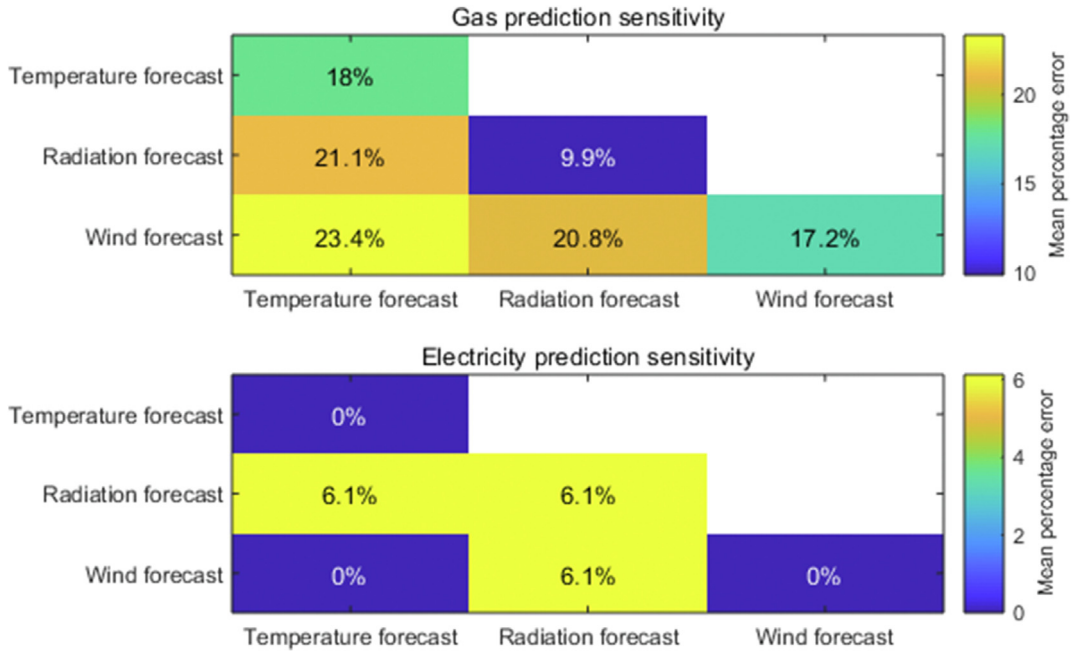

Fig. 10 – A heatmap of the local discrete sensitivities (Eq. (19)) of the predicted power and gas usage to weather forecast error.

to the second order interactions of errors in forecast variables.

4. Discussion

This study investigates the role of weather forecast error on greenhouse energy demand prediction and power trading. Additionally, this study considers the impact of each forecasted weather variable and how power trading is impacted when using multiple markets. This study uses a method that is not validated as part of this studies analysis but provides novel and relevant insight into the management of energy in greenhouses.

This study explores how weather forecast errors can result in the misprediction of both gas and power demand in a greenhouse. In this specific study, the prediction uncertainty suggests an overprediction of the gas and power demand of the greenhouse. The overprediction of energy demand is linked to the notable negative bias in the temperature and global radiation forecast errors (Fig. 5). As a result, the amount of available natural heat and radiation is being consistently underestimated and as a result excess gas and power is being bought to meet this perceived deficit (Fig. 6). It should be noted that the overprediction of the greenhouse energy demand in this study is case specific and it is entirely possible for different weather forecasts to produce alternate patterns of misprediction. However, this study demonstrates that the effects of misprediction can be large. The analysis also concludes that the cumulative amount of energy being mispredicted increased with the weather forecast prediction horizon length, corroborating the conclusions of Tap et al. (1996). This is understandable as longer forecasts should become progressively more uncertain. The conclusions made on the volume of the predicted energy demand were made using a winter dataset and have not been extrapolated to the whole year. This is as the winter is the season of the highest use of artificial lighting in practice and requires more power than the rest of the year.

The sensitivities of the energy predictions to weather forecast variables showed that gas prediction is sensitive to wind and temperature forecast error while power prediction is sensitive to the global radiation forecast error (Fig. 10). This observation is due to the fact that the global radiation forecast directly influences the need for supplementary artificial lighting and therefore the power demand. Gas is used to provide heat and its demand depends on heat moving through the greenhouse based on the temperature gradient between the inside and outside temperature and the convective energy transported through the greenhouse shell. The dependence of gas use prediction error on the temperature forecast and not the global radiation forecast may be because the data set used in the study was from a Dutch winter where the ambient radiation levels are low. In summer one would expect that both the outside radiation and temperature would have a large effect on gas demand prediction as solar radiation is a key source of natural heat in the greenhouse. These results were calculated using 48-h long weather forecasts and as such this assumption excludes how these sensitivities might change over varying weather forecast prediction horizon lengths. While this does provide an opening for future research this study has shown that the broad trends and biases in the weather forecast error are consistent for all horizon lengths. Consequently, it is anticipated that the conclusions of this analysis would be broadly consistent for all horizon lengths.

The power trading uncertainty analysis included in this paper offers a number of key insights into how weather forecast error might affect the power trading process and economic efficiency of the greenhouse. Most prominently, the corrective trading of mispredicted power can impact the economic performance of the greenhouse. This impact arises from the fact that although the volume of power being traded in corrective bidding is relatively smaller than the initial trade (Fig. 8), the corrective imbalance price is more volatile (Fig. 7). This can lead to the grower risking a higher price for their power than if it had been bought correctly in the initial trade. In this way it is better to reduce the impact of weather forecast error to mitigate the risk of volatile short-term prices.

Additionally, the power trading analysis confirmed the conclusion of Sigrimis et al. (2001), in that the inclusion of forecast errors increases the operating costs of a greenhouse. Moreover, these costs worsen with the increasing length of the weather forecasts as can be seen by the increase in the mean costs for both the initial and corrective trading (Fig. 9). Subsequently shorter weather forecasts would be preferable for minimising error. Interestingly the standard deviation of the initial and corrective power demand decreases as the forecast horizon increases. A hypothesis is that the errors tend to cancel out when summed over longer periods. So, a large deviation from the mean is less probable for a long prediction horizon. An analysis should be performed with a larger dataset for more reliable conclusions to be drawn. It should also be noted that the markets used are Dutch and conclusions may vary based on the region of the market used. Another interesting observation is that the standard deviation of the corrective power demand costs (Fig. 9) rises to a peak at a 72 h long forecast and then decreases. This is a potential result of a combination of lower prediction error at shorter forecast lengths and a cancellation of costs at longer forecasts lengths. Indeed, this happened in the corrective costs and not the initial costs as the price distribution for the day-ahead market has a greater bias to positive values, whereas the imbalance price is more centred on zero and takes negative values more frequently, as can be seen in Fig. 7.

While this method is simple to apply it calculates the prediction error directly, without the assumptions related to the initial distribution of the weather forecast error that have been used in previous studies (Seginer et al., 2018; Su, Xu, & Goodman, 2017b). Thus, the conclusions drawn from this method are inexorably linked to the weather forecast dataset as they are so spatially and temporally specific. While this specificity makes conclusions difficult to generalise it could be done using large or varied forecast datasets and multiple greenhouse models. Despite this the use of direct comparison of energy predictions in this method means that it can be applied other greenhouse systems and model formats and offer the same analysis. Moreover, this method can be applied to data from any place or time and produce relevant insight.

This study does not include outside CO_2 data but assumes it is constant, this presents limitations to the conclusions regarding energy consumption as one use of a CHP is to provide supplementary CO_2, which in turn is dependent on the outside conditions. The operation of the CHP for this purpose also affects the greenhouse energy demand due to the power and heat that is also produced. The inclusion of outside CO_2 data may offer insight into how the CHP is operated based on motives other than power demand and how that might affect selling surplus power to the grid. As this study is conducted in winter when the demand for supplementary CO_2 is less, it is anticipated that this surplus power will be relatively minor when compared to the power trading discussed in this study.

A limitation of this study is that the economic analysis uses the imbalance market price for the short-term trading of power. While the imbalance price has been used in previous research (van Beveren et al., 2019) it is more common in practice to use the intra-day market price. Despite this limitation the conclusions of this study are relevant as the imbalance and intra-day markets are comparable representations of short-term power prices.

The possible practical consequences of energy demand prediction error and the subsequent power trading are that grower may lose economic efficiency by having to trade on the more volatile short-term markets. These short-term markets are often supplied by immediately accessible power, often originating from fossil fuels. As a result, decreasing the corrective power trading of a greenhouse may also help reduce its carbon footprint. To try and achieve this the weather forecast bias could be accounted for in the energy prediction and energy buying process. This would need to have a highly localised approach as the variations in local climate strongly influence the validity of the global radiation forecast as demonstrated by Doeswijk and Keesman (2005).

Additionally, the insight from the sensitivity analysis presents an opportunity to improve the data collection and screening process by identifying weather forecast data with errors that disproportionally impact the uncertainty of model prediction. In particular this study's conclusion that the global radiation forecast is a key cause of power misprediction parallels the importance of accounting for the error in radiation sensors found in Bontsema, van Henten, Gieling, and Swinkels (2011). This type of insight can drive more efficient energy consumption in the horticultural sector, but also extends to any facility that uses weather forecasts to define its climate and energy buying strategy, such as food storage warehouses and offices.

5. Conclusion

To conclude, this study investigates the role of weather forecast uncertainty and its effect on greenhouse energy demand prediction and power trading. This was done through the direct comparison of predictions made with weather recordings and forecasts. The economic analysis of power trading was done using multiple markets to quantify the costs more realistically.

This study shows a clear bias in the prediction of gas and power demand to buy more than is necessary when using a weather forecast. This bias is linked to the high sensitivity of the energy predictions to underestimate of temperature and global radiation in the forecasts in this study. The error present in weather forecasts and in greenhouse energy demand predictions do increase with longer weather forecast prediction horizon lengths. The power trading analysis concluded that while the volume of initial trading was greater than the

corrective trading, the higher volatility in short term Imbalance market prices can result in higher costs per unit of power. Additionally, the means of the demand and cost of both initial and corrective demand increase with the forecast horizon prediction length. A sensitivity analysis was done on the weather forecast variables and concluded that in the Dutch winter case the global radiation forecasts have the greatest impact on power prediction error (6.1%), whereas gas demand prediction is strongly influenced by the wind (18.0%) and outside temperature forecast (17.2%).

Funding

This work is part of the research programme FlexCrop with the project number 647.003.006, which is (partly) financed by the Dutch Research Council (NWO) and the companies, AgroEnergy, Blue Radix, B-Mex, LTO Glaskracht Nederland, Letsgrow.com, WUR Greenhouse Horticulture and Delphy.

Declaration of competing interest

The authors declare that they have no known competing financial interests or personal relationships that could have appeared to influence the work reported in this paper.

Acknowledgments

We thank Gert-Jan Swinkels of Wageningen Research, business unit Greenhouse Horticulture, for technical support and valuable discussions on using the online version of KASPRO (de Zwart, 1996; Dieleman et al., 2005; Elings et al., 2006; Luo, de Zwart et al., 2005; Luo, Stanghellini, et al., 2005) for this study. We would also like to thank the reviewers for the constructive feedback to improve the quality of this paper.

Appendix A. Cloudiness index and ambient CO_2 level sensitivity analysis

A Sobol sensitivity analysis (Saltelli et al., 2008) was performed to assess the impact of the assumptions made about the weather data used in this study. The assumptions that are included are (Table 3) that the cloudiness index (CI) is constant at 0.7 and that the Outdoor $C0_2$ level ($C0_{2_{out}}$) is constant at 410 ppm.

To perform a sensitivity analysis, the parameter $C0_{2_{out}}$ has a normal prior distribution defined. Its mean is the nominal value used in the study, with a standard deviation (*s.d*) defined so that the 99th percentile of the prior is approximately ±10% of the mean value:

$$s.d = (0.1*mean) / 5 \quad (20)$$

The cloudiness index parameter (CI) has a prior distribution that is defined as a uniform distribution. This distribution shape and limits are chosen based on expert opinion and the distribution of historical cloudiness index data. The limits of this prior are defined as being between 0.4 and 0.8.

Table A3 – Parameter priors used in the assumption sensitivity analysis

	Normal distribution		Uniform distribution
	Outdoor $C0_2$ ($C0_{2_{out}}$)		Cloudiness index (CI)
Mean	410	Min	0.4
Standard deviation	8.20	Max	0.8
Assumed value	410		0.7

These parameter distributions are sampled 1000 times using a Monte-Carlo method. This set of samples are used to simulate 1000 greenhouse power demand predictions using the KASPRO model and recorded weather data setup described in Sections 2.1–2.8.

These simulations when used in the Sobol sensitivity framework concluded that the prediction of greenhouse power demand is completely insensitive to variations in the two parameters included in this analysis. This result is logical as within KASPRO the greenhouse power demand is derived from the lamp lighting power demand and the parameters $C0_{2_{out}}$ and CI are not included in the control of the lamp lighting. In the case of the CI, this parameter is used to calculate the diffuse radiation but a separate data stream, the global radiation, is used to control the lighting. This means that while the values used in these assumptions should be realistic, their precise value has no impact on the analysis done in this study.

REFERENCES

Bontsema, J., van Henten, E. J., Gieling, T. H., & Swinkels, G. L. A. M. (2011). The effect of sensor errors on production and energy consumption in greenhouse horticulture. *Computers and Electronics in Agriculture, 79*(1), 63–66. https://doi.org/10.1016/j.compag.2011.08.008

Chalabi, Z. S., Bailey, B. J., & Wilkinson, D. J. (1996). A real-time optimal control algorithm for greenhouse heating. *Computer and Electronics in Agricutlure, 15*(1), 1–13. https://doi.org/10.1016/0168-1699(95)00053-4

de Zwart, H. F. (1996). *Analysis energy-saving options in greenhouse cultivation using a simulation model* (Ph.D Thesis). Landbouwuniversiteit Wageningen.

Dieleman, J. A., Meinen, E., Marcelis, L. F. M., de Zwart, H. F., & van Henten, E. J. (2005). Optimisation of CO2 and temperature in terms of crop growth and energy use. *Acta Horticolturae, 691*, 149–154. https://doi.org/10.17660/ActaHortic.2005.691.16

Doeswijk, T. G., & Keesman, K. J. (2005). Adaptive weather forecasting using local meteorological information. *Biosystems Engineering, 91*(4), 421–431. https://doi.org/10.1016/j.biosystemseng.2005.05.013

Doeswijk, T., Keesman, K. J., & Van Straten, G. (2006). Impact of weather forecast uncertainty in optimal climate control of storehouses. In *4th IFAC workshop on control applications in post-harvest and processing technology, Bornimer Agrartechnische Berichte* (pp. 46–57). Potsdam.

Elings, A., de Zwart, H. F., Janse, J., Marcelis, L. F. M., & Buwalda, F. (2006). Multiple-day temperature settings on the basis of the assimilate balance: A simulation study. *Acta Horticulturae, 718*, 219–226. https://doi.org/10.17660/ActaHortic.2006.718.24

Golzar, F., Heeren, N., Hellweg, S., & Roshandel, R. (2021). Optimisation of energy-efficient greenhouses based on an integrated energy demand-yield production model. *Biosystems Engineering, 202*, 1–15. https://doi.org/10.1016/j.biosystemseng.2020.11.012

Gutman, P., Lindberg, P., Ioslovich, I., & Seginer, I. (1993). A non-linear optimal greenhouse control problem solved by linear programming. *Journal of Agricutlural Engineering*, 55(4), 335–351. https://doi.org/10.1006/jaer.1993.1054

Keesman, K. J., Peters, D., & Lukasse, L. J. S. (2003). Optimal climate control of a storage facility using local weather forecasts. *Control Engineering Practice, 11*(5), 505–516. https://doi.org/10.1016/S0967-0661(02)00144-2

Kuijpers, W. J. P., Katzin, D., van Mourik, S., Antunes, D. J., Hemming, S., & van de Molengraft, M. J. G. (2021). Lighting systems and strategies compared in an optimally controlled greenhouse. *Biosystems Engineering, 202*, 195–216. https://doi.org/10.1016/j.biosystemseng.2020.12.006

Luo, W., de Zwart, H. F., DaiI, J., Wang, X., Stanghellini, C., & Bu, C. (2005). Simulation of greenhouse management in the subtropics, Part I: Model validation and scenario study for the winter season. *Biosystems Engineering, 90*(3), 307–318. https://doi.org/10.1016/j.biosystemseng.2004.11.008

Luo, W., Stanghellini, C., Dai, J., Wang, X., de Zwart, H., & Bu, C. (2005). Simulation of greenhouse management in the subtropics, part II: Scenario study for the summer season. *Biosystems Engineering, 90*(4), 433–441. https://doi.org/10.1016/j.biosystemseng.2004.12.002

Orgill, J. F., & Hollands, K. G. T. (1977). Correlation equation for hourly diffuse radiation on a horizontal surface. *Solar Energy, 19*(4), 357–359. https://doi.org/10.1016/0038-092X(77)90006-8

Saltelli, A., Ratto, M., Andres, T., Campolongo, F., Cariboni, J., Gatelli, D., et al. (2008). *Global Sensitivity analysis. The primer*. Chichester: John Wiley & Sons. https://doi.org/10.1002/9780470725184

Seginer, I., Ioslovich, I., & Albright, L. D. (2006). Improved strategy for a constant daily light integral in greenhouses. *Biosystems Engineering, 93*(1), 69–80. https://doi.org/10.1016/j.biosystemseng.2005.09.007

Seginer, I., & McClendon, R. (1992). Methods for optimal control of the greenhouse environment. *American Society of Agricultural Engineers, 35*, 1299–1307. https://doi.org/10.13031/2013.28733

Seginer, I., van Beveren, P. J. M., & van Straten, G. (2018). Day-to-night heat storage in greenhouses: 3 Co-generation of heat and electricity (CHP). *Biosystems Engineering, 172*, 1–18. https://doi.org/10.1016/j.biosystemseng.2018.05.006

Seginer, I., van Straten, G., & van Beveren, P. J. M. (2017). Day-To-night heat storage in greenhouses: A simulation study. *Acta Horticulturae, 1182*, 119–127. https://doi.org/10.17660/ActaHortic.2017.1182.14

Sigrimis, N., Ferentinos, K. P., Arvanitis, K. G., & Anastasiou, A. (2001). A comparison of optimal greenhouse heating setpoint generation algorithms for energy conservation. *IFAC Proceedings Volumes, 34*(11), 61–66. https://doi.org/10.1016/S1474-6670(17)34107-1

Statistics Netherlands [Internet]. (2021). Horticulture underglass cultivation census. Retrieved November 2, 2020, from https://opendata.cbs.nl/statline/portal.html?_la=en&_catalog=CBS&tableId=80783eng&_theme=1107.

Su, Y., Xu, L., & Goodman, E. D. (2017a). Greenhouse climate fuzzy adaptive control considering energy saving. *International Journal of Control, Automation and Systems*, 15(4), 1936–1948. https://doi.org/10.1007/s12555-016-0220-6

Su, Y., Xu, L., & Goodman, E. D. (2017b). Nearly dynamic programming NN-approximation-based optimal control for greenhouse climate: A simulation study. *Optimal Control Applications and Methods*, 1–25. https://doi.org/10.1002/oca.2370

Su, Y., Xu, L., & Goodman, E. D. (2021). Multi-layer hierarchical optimisation of greenhouse climate setpoints for energy conservation and improvement of crop yield. *Biosystems Engineering, 205*(1180), 212–233. https://doi.org/10.1016/j.biosystemseng.2021.03.004

Tap, F., van Willigenburg, L. G., & van Straten, G. (1996). Receding horizon optimal control of greenhouse climate based on the lazy man weather prediction. In *Proc. Of 13th IFAC World Congress, San Francisco* (pp. 387–392). https://doi.org/10.1016/S1474-6670(17)57776-9

Vadiee, A., & Martin, V. (2012). Energy management in horticultural applications through the closed greenhouse concept, state of the art. *Renewable and Sustainable Energy Reviews, 16*(7), 5087–5100. https://doi.org/10.1016/j.rser.2012.04.022

Vanthoor, B. H. E., Stigter, J. D., van Henten, E. J., Stanghellini, C., Visser, P. H. B. De, & Hemming, S. (2012). A methodology for model-based greenhouse design : Part 5 , greenhouse design optimisation for southern-Spanish and Dutch conditions. *Biosystems Engineering, 111*(4), 350–368. https://doi.org/10.1016/j.biosystemseng.2012.01.005

van der Velden, N., & Smit, P. (2021). *Energiemonitor van de Nederlandse glastuinbouw 2020. (Wageningen economic research rapport; No. 2021-127)*. Wageningen: Wageningen Economic Research. https://doi.org/10.18174/505786

van Beveren, P. J. M., Bontsema, J., van Straten, G., & van Henten, E. J. (2019). Optimal utilization of a boiler, combined heat and power installation, and heat buffers in horticultural greenhouses. *Computers and Electronics in Agriculture, 162*, 1035–1048. https://doi.org/10.1016/j.compag.2019.05.040

van Beveren, P. J. M., Bontsema, J., van 't Ooster, A., van Straten, G., & van Henten, E. J. (2020). Optimal utilization of energy equipment in a semi-closed greenhouse. *Computers and Electronics in Agriculture, 179*. https://doi.org/10.1016/j.compag.2020.105800

van Henten, E. J., & Bontsema, J. (2009). Time-scale decomposition of an optimal control problem in greenhouse climate mmanagement. *Control Engineering Practice, 17*, 88–96. https://doi.org/10.1016/j.conengprac.2008.05.008

van der Meer, D., Widén, J., & Munkhammar, J. (2018). Review on probabilistic forecasting of photovoltaic power production and electricity consumption. *Renewable and Sustainable Energy Reviews, 81*, 1484–1512. https://doi.org/10.1016/j.rser.2017.05.212

van Ooteghem, R. J. C. C. (2010). Optimal control design for a solar greenhouse. *IFAC Proceedings Volumes, 43*(26), 304–309. https://doi.org/10.3182/20101206-3-JP-3009.00054

Vogler-Finck, P., Bacher, P., & Madsen, H. (2017). Online short-term forecast of greenhouse heat load using a weather forecast service. *Applied Energy, 205*, 1298–1310. https://doi.org/10.1016/j.apenergy.2017.08.013

Wang, Y., Mao, S., & Nelms, R. (2015). *Online algorithms for optimal energy distribution in microgrids*. Springer. https://doi.org/10.1007/978-3-319-17133-3